

The Effect of CO₂ Coinjection on Silica Scaling in Acid Dosed Subduction Zone Geothermal Brines

*Akira Kamiya^{1,2}, Pedro Rendel², Bruce Mountain², Alexander Nichols¹, and Mark Jermy³

¹School of Earth and Environment, University of Canterbury, New Zealand

²GNS Science, Wairakei Research Centre, New Zealand

³Department of Mechanical Engineering, University of Canterbury, New Zealand

* a.kamiya@gns.cri.nz

Keywords: *Carbon emissions, non-condensable gas, CO₂ reinjection, silica scale.*

ABSTRACT

Geothermal energy is not inherently carbon neutral; it releases non-condensable gases (NCG) during energy production. Although geothermal energy is a strong contender in the low-carbon energy space, it must reduce these emissions to compete effectively with other renewable energy sources. For this reason, capturing and reinjecting NCG is an emerging method being implemented and considered by the geothermal industry.

However, carbon emissions are not the only concern in geothermal energy production. Another common issue faced by the geothermal industry is silica scaling. At the interface between the reinjection brine and reservoir rock, shifts in pH can cause amorphous silica scale to form. Previous research has suggested that the co-injection of CO₂ with acid-dosed brines may help inhibit this scaling.

To investigate this potential solution, we conducted two reinjection simulation experiments using a high-pressure and high-temperature (HPHT) flow-through system to replicate conditions typical of island-arc geothermal systems, such as those in Japan, Indonesia, and The Philippines. The significant geothermal energy potential in these regions makes studying these systems essential. In the experiments, we used a synthetic geothermal brine and exposed it to andesite + calcite.

Our results indicate that adding CO₂ to acid-dosed brines can significantly reduce the rate of silica scaling in the reservoir. In our experiments, introducing 2000 ppm CO₂ into the fluid maintained a low pH solution, resulting in almost no scaling—a stark contrast to the outcomes observed without adding CO₂. These results suggest that the co-injection of CO₂ in geothermal power plants will be beneficial in reducing plant emissions while at the same time mitigating silica scaling within the reservoir.

1. INTRODUCTION

Geothermal energy will be an integral part of the transition to net-zero carbon emissions. However, the extent to which it will replace fossil fuel usage remains to be determined. Geothermal energy generation is not inherently carbon neutral, as non-condensable gases (NCG) dissolved in the geothermal fluid are often released during energy generation. These emissions primarily consist of CO₂, with smaller amounts of H₂S, and trace quantities of H₂, CH₄, NH₃, N₂, and Ar.

Typically, these gases are released into the atmosphere. While the emission of these gases is a natural process in all geothermal systems, the geothermal industry must aim to

minimise these emissions to be competitive with other low-carbon energy sources and serve as an adequate substitute for fossil fuels.

More recently, power plant operators have started to implement and consider the co-injection of NCG, primarily CO₂, with reinjection fluids. Although this method does not achieve the sequestration of CO₂ over geologically significant periods, it can offset immediate and more localised CO₂ emissions. To date, the reinjection of CO₂ has been implemented with varying degrees of success (see Kaieda et al., 2009; Nagl, 2010; Yanagisawa, 2010, as cited in Kaya & Zarrouk, 2017). A prominent example of successful CO₂ reinjection is the Ngawha Power Station in New Zealand. Despite previously being one of the country's highest CO₂ emitters (OEI of 162 gCO₂eq/kWh(net) as of CY 2022), reinjection has enabled it to become one of New Zealand's first zero-carbon operators (Montague et al., 2023).

However, CO₂ emissions are not the only concern in geothermal energy extraction. Mineral scaling, most commonly of amorphous silica, is a primary issue in almost all geothermal power production operations. This is especially true when brines contain a high concentration of silica. Amorphous silica scaling occurs when silica, previously dissolved in geothermal fluids, precipitates on plant equipment and within the reservoir or well. Extensive scaling in the reservoir can reduce porosity and permeability, reducing injectivity and overall plant efficiency (Luo et al., 2023).

As silica precipitation rate is reduced at lower pH values, a common practice involves acid-dosing the geothermal brine. Although this method essentially prevents scaling on plant equipment, it often fails to inhibit scaling within the reservoir. When reinjection fluids encounter reservoir rocks, they can react with various minerals, neutralising the pH. This can cause particularly prolific scaling in the area surrounding the reinjection well. Furthermore, when the reservoir formation contains calcite, the pH shift can be extreme, exacerbating the problem of scaling.

Recent research at GNS Sciences' Experimental Geochemistry Laboratory (EGL) investigated the effect of CO₂ co-injection in a typical New Zealand geothermal system. In this study, greywacke + calcite were exposed to New Zealand geothermal brine with varying concentrations of CO₂. The results demonstrated that CO₂ successfully inhibited silica scaling (Mountain, *pers comm*).

Building on this work, we report the results of experimental work exploring the applicability of these findings to island-

arc geothermal environments, such as those in Japan, Indonesia, and The Philippines. These regions collectively represent a significant portion of the global geothermal energy potential, with Indonesia alone estimated to hold 35-40% of the world's geothermal resources (Fan & Nam, 2018; Nasruddin et al., 2016). Given the vast potential in this region, it is crucial to investigate the applicability of this technology.

In island-arc settings, the lithologies and fluids differ from those in New Zealand, making it essential to understand how these differences might impact the effectiveness of CO₂ co-injection as a scaling deterrent. Of particular concern is the significantly higher Ca concentration, which, when combined with sulphate in the solution, may pose a risk of anhydrite precipitation.

Our study employs an experimental approach to simulate the fluid-rock interactions between andesite (the predominant reservoir rock in Indonesian geothermal systems; Purnomo & Pichler, 2014) and high-salinity brines containing CO₂. By doing so, we aim to assess the viability of CO₂ co-injection in these geothermal systems.

2. METHODOLOGY

Two experimental reinjection simulations (Table 1) are presented here that studied the effect of adding CO₂ to acid-dosed brines during reinjection. We used andesite combined with a controlled amount of calcite and synthetic geothermal brine.

The rock used was a fresh, unaltered medium-K type andesite, identified as the Waitoa Andesite, and was collected from the central Hauraki Plains, approximately 40 km northeast of Hamilton, New Zealand (Rosenburg, 2010). XRD analysis shows quartz, tridymite, pyroxene, and andesine are primary minerals. Andesite is used in these experiments because island arc settings, such as those in the Philippines and Indonesia, are typified by andesite-hosted volcanic systems (Defant et al., 1990; Purnomo & Pichler, 2014; Stimac et al., 2008; Sussman et al., 1993).

The brine used in this experiment was synthetic and was prepared based on available chemistry data from a reinjection fluid collected at a geothermal power station in Indonesia. High concentrations of Ca, Cl, Na, and K characterise this brine. The brine was acid-dosed using

concentrated sulfuric acid to best replicate real-world reinjection scenarios.

Table 1: Rock type and CO₂ concentration of the two experiments.

Experiment no.	Rock type	CO ₂ concentration
Experiment 1	Waitoa andesite + 1.5 wt.% calcite	No CO ₂
Experiment 2	Waitoa andesite + 1.5 wt.% calcite	2000 ppm CO ₂

The experimental apparatus used in this study consists of a high-pressure and high-temperature (HPHT) titanium alloy flow-through reactor (Figure 1). This system enables a continuous single-pass flow of fluid through a rock medium at elevated temperatures (up to 400°C) and pressures (up to 500 bar), thereby able to simulate conditions comparable to those at the reinjection site of a geothermal power station.

Continuous flow is facilitated by a double-piston metering pump (Figure 1), which is controlled by a connected computer to set the flow rate in the range of 0.001 to 15 ml/min. For these experiments, the flow rate was set to 5 ml/min.

Two titanium pressure vessels were used to simulate the reinjection process. The first pressure vessel (the Preheater) heats the fluid to 250°C and is used to depolymerise silica in the brine. The fluid then travels to the next pressure vessel (the Reactor), interacting with the rock. After this, the fluid passes through a digital back pressure regulator and is collected in a disposable syringe.

In both experiments, the fluid was deoxygenated before being placed in the system. In the experiments where CO₂ was added, the volume of CO₂ required to achieve the desired concentration in one litre of the brine was calculated using the ideal gas law equation.

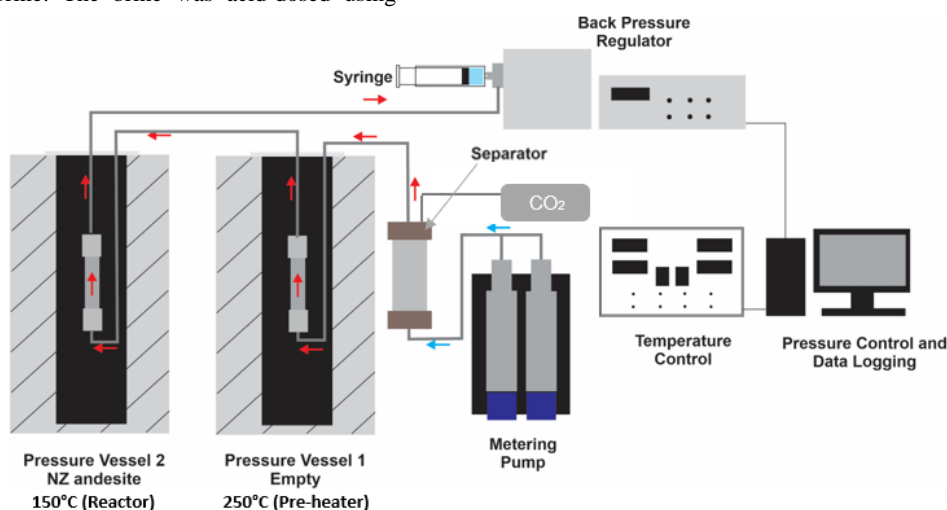


Figure 1: High temperature and pressure hydrothermal flow simulator (Coretest Systems Ltd) located at the EGL atGNS Science Wairakei site. Modified from Sajkowski et al. (2022).

Each experiment lasted 31 days, beginning with an initial three-day period, during which the Reactor was kept at room temperature to remove O₂ and check for leakages. For the subsequent 28 days, the Reactor was heated to the experimental temperature of 150°C. The Preheater was at 250°C for the entire duration of the experiments.

Fluid samples were collected daily and analysed for a range of elements using Inductively Coupled Plasma Optical Emission Spectrometry (ICP-OES), Ion Chromatography (IC), UV-Vis Spectroscopy, and HCO₃ Titration. At the end of each experiment, the rock in the Reactor was removed and studied using Scanning Electron Microscopy with Energy Dispersive Spectroscopy (SEM-EDS) analyses.

3. RESULTS

The results from the two reinjection simulation experiments are presented in Figures 2a-f.

3.1 Andesite + 1.5 wt.% calcite, no CO₂

This experiment served as a control to observe the interaction between the reinjection fluid and andesite in the presence of calcite but no added CO₂.

The first two samples were collected when the Reactor was at room temperature. The input brine had a pH of 4.5, which increased to 6.42 in the first sample. The concentration of SiO₂ in the effluent sample was 554 ppm in the second sample, down from the input value of 850 ppm, before increasing to 636 ppm by the end of the room temperature period.

Components such as As, Mg, Mn, Li, and Zn became detectable during the room temperature period, despite not being present in the input brine. Furthermore, CO₂ measurements reached 109 ppm. All other components showed concentrations that did not differ significantly from those in the input brine.

Shortly after the Reactor was heated to the experimental temperature (150°C), the pH_T (temperature-adjusted pH) spikes, reaching a maximum value of 6.75 in the fifth sample. After this peak, the pH_T of the effluent decreased relatively steadily, reaching 5.49 by the end of the experiment.

SiO₂ concentration dipped slightly after the temperature increased to 150°C, decreasing to 597 ppm, but then increased over the subsequent samples to 750 ppm by the eighth sample. Although the SiO₂ concentration fluctuated slightly, it was generally lower than the input value throughout the experiment, ending at 641 ppm after 31 days. This suggests that silica loss was most pronounced at the start of the experiment when the fluid interacted with the fresh rock. Once the concentration stabilised, silica loss appeared to be lower in the middle section, then increased again towards the end of the experiment. During this experiment, a blockage within the input pipe was observed on two occasions, which had to be manually cleared.

The concentrations of Ca, Na, and K show nearly identical trends, remaining similar to the input solution for the first

half of the experiment (approximately until day 14) but show minor increases towards the end of the experiment.

SO₄ concentrations remained relatively stable throughout the experiment, with a small peak observed in the middle.

It is difficult to discern significant trends from the CO₂ data due to the difficulties with preservation when collecting the samples. However, measurable concentrations of CO₂ were present in almost all effluent samples.

SEM-EDS analyses of the reacted grains (3c, d) reveal clear evidence of silica scaling, particularly at the bottom of the Reactor where the fluid first interacts with the rock (Figure 3d). Scaling decreases towards the top of the Reactor, where the fluid exits. Calcite grains are almost entirely covered with silica scale throughout the Reactor. Scaling on all grains makes it difficult to identify any alteration.

3.2 Andesite + 1.5 wt.% calcite, 2000 ppm CO₂

This experiment investigated the effect of adding CO₂ to the reinjection fluid on the silica scaling rate. The same methodology and conditions were used, with the only difference being the addition of 2000 ppm of CO₂ to the fluid.

Similar to the previous experiment, the first two samples represent the room-temperature period. The pH of the input fluid was lower than in the previous experiment, averaging 3.86. This is due to the high CO₂ content. The pH increased to 5.65 in the first sample and stabilises at 5.64 by the end of the room-temperature period. The concentration of SiO₂ decreased slightly from approximately 840 ppm in the input solution to ~780 ppm during the room-temperature period. As with the previous experiment, As, Mg, Mn, Li, and Zn were detected in the effluent, despite being absent in the input solution.

Ca concentrations, initially around 470 ppm in the input solution, rose by nearly 200 ppm during the room-temperature period to 650 ppm. SO₄ concentrations were initially just 5 ppm lower than in the input solution (21 ppm on Day 2) but decreased to almost half the input level by Day 3 (14 ppm). The concentrations of most other major components do not differ significantly from the input solution during the room-temperature period.

Once the Reactor was heated to 150°C, the in-situ pH (pH_T) increased, reaching a maximum value of 5.73. After this initial increase, the pH_T decreased relatively steadily, reaching 4.30 by the end of the experiment.

The SiO₂ concentration was lowest immediately after the temperature increase, at 705 ppm, then rapidly increased to 802 ppm by the seventh sample. A small but stable increase in SiO₂ concentration continued until Day 15, when it reached 846 ppm and stabilised. At this point, no further silica losses were observed relative to the input solution.

Upon temperature increase, SO₄ concentrations remained around 14 ppm (approximately half that of the input solution) until Day 12. Afterwards, the concentration stabilised at a slightly higher value of 18 ppm, where it remained for the rest of the experiment.

The concentrations of other elements, including Ca, K, and Na, show little to no change from the composition of the blanks and remained relatively stable throughout the experiment.

Trends in the CO₂ data are difficult to discern, likely due to challenges in preserving CO₂ in the samples.

SEM-EDS analyses of the reacted grains reveal effectively no scaling throughout the Reactor (Figure 3a, b). Additionally, no calcite was present in the Reactor at the end of the experiment. Some alteration of the primary minerals was observed on the grains, particularly towards the bottom of the Reactor, with the appearance of suspected clay minerals. Finally, there was little to no difference in surface composition (as determined by EDS) relative to the unreacted grains.

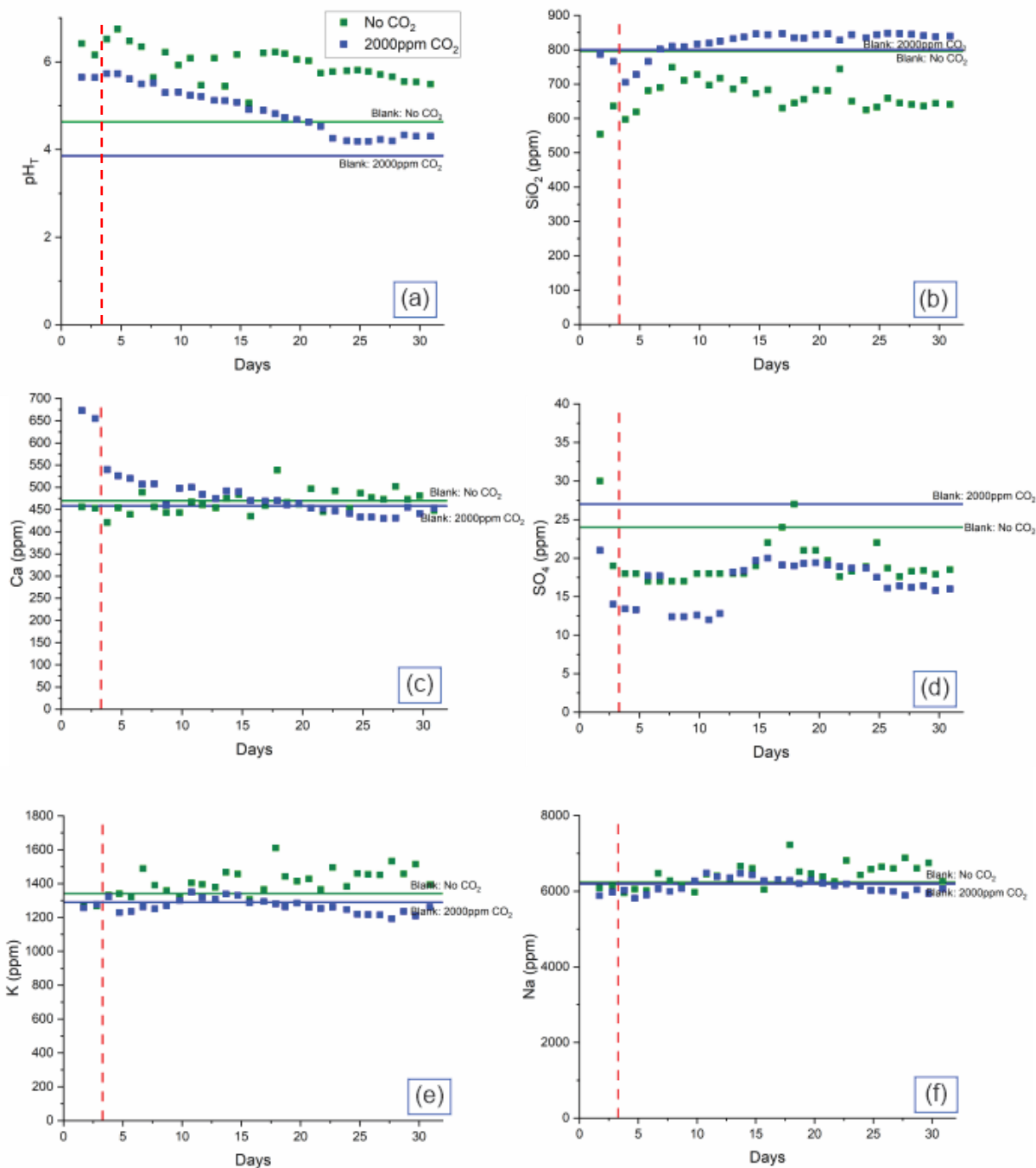


Figure 2a-f: Effluent chemistry from the two experiments plotted versus time in days. The green points show the results from the experiment without CO₂ in the fluid, while the blue points are from the experiment with 2000 ppm of CO₂ added to the solution. The vertical red dashed line shows the point where the Reactor was heated to 150°C.

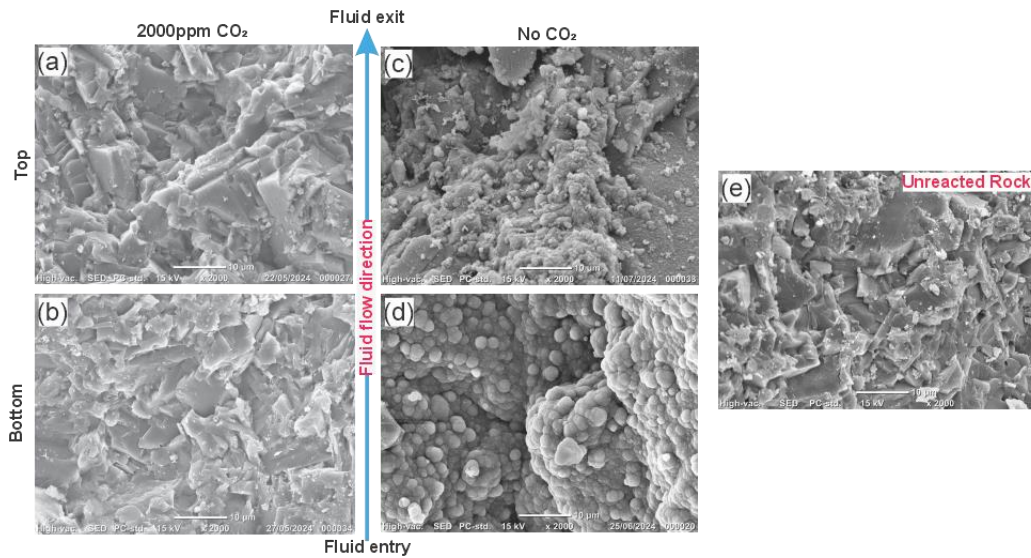
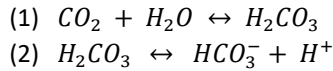


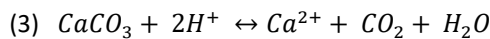
Figure 3a-e: Backscatter electron photomicrograph of reacted andesite grains. (a) and (b) are reacted grains from the 2000 ppm CO₂ experiment, while (c) and (d) are from the experiment without CO₂. (a) and (c) are from the top of the Reactor (near the fluid exit point) in the respective experiments, while (b) and (d) likewise represent the grains at the bottom of the Reactor (near the fluid entry point). (e) shows an unreacted grain.

4. DISCUSSION

The addition of CO₂ to the fluid results in the pH decreasing in accordance with the following reactions:



While these reactions decrease the fluid pH, interactions with the rock increase pH. Specifically, the interaction between the acidified fluid and carbonate minerals (including calcite). Calcite dissolves in acid according to the following equation:



This reaction produces CO₂, consumes H⁺, and increases Ca concentration in the fluid. Additionally, the dissolution of minerals like feldspars can alter the fluid pH and release cations into the fluid. Fine rock material, leftover from crushing the rock may accelerate this process at the start of the experiment. As H⁺ is consumed, H₂CO₃ dissociates to replace it, thus buffering the pH.

The pH buffering observed in both experiments can be attributed to these reactions, where acidity is neutralised by interaction with calcite and other minerals in the andesite. In the experiment without CO₂, calcite dissolution is confirmed by the presence of CO₂ in the effluent samples. In the experiment with 2000 ppm of CO₂, the spike in Ca observed early indicates calcite dissolution. This suggests that almost all calcite was consumed in 16 - 20 days, after which Ca concentrations returned to levels similar to those in the input solution. Furthermore, no calcite was found at the end of the experiment with 2000 ppm CO₂, suggesting it had all been dissolved. This is noteworthy as it suggests that, with sufficient time, the addition of CO₂ helps to 'clean' the area immediately surrounding the fluid-rock interface of calcite.

The pH results from the experiment without CO₂ are significantly higher than the experiment with CO₂, indicating that adding CO₂ can suppress the pH shift caused by calcite dissolution. Despite not reaching the pH value observed in the experiment with CO₂, the experiment without CO₂ exhibits a minor downward trend in pH. This could be related to the armouring of the grains (particularly calcite) surface with SiO₂, which reduces the exposed surface area of the rock. This is supported by the extensive scaling on the surface of the calcite grains observed in the SEM-EDS analysis.

SiO₂ loss is notably reduced when CO₂ is added to the solution; in fact, there is no SiO₂ loss relative to the input solution by the end of this experiment. This can be attributed to the low pH maintained by adding CO₂. The absence of SiO₂ loss from the fluid suggests limited silica scaling, which was confirmed by SEM-EDS observations of the rock. In contrast, the experiment without CO₂ showed consistent SiO₂ loss relative to the input solution, with extensive silica scaling on the rock surface observed in SEM-EDS analysis.

Mineral saturation indices (SI), calculated using Geochemists Workbench (GWB; Bethke, 2022; Bethke et al., 2018; Bethke et al., 2020; Bethke et al., 2024), are shown for amorphous silica, anhydrite, and calcite (Figure 4a-c). These graphs show that despite the lack of scaling observed in the SEM for the CO₂-containing experiment, SiO₂ (amorphous) remained slightly supersaturated throughout the experiment ($\log(Q/K) > 0$). This was also true for the experiment without CO₂. Anhydrite, a concern due to the presence of SO₄ and high concentrations of Ca in the solution, as well as its retrograde solubility, remained undersaturated throughout both experiments. Calcite also

remains undersaturated for the majority of samples in both experiments.

Ca-Na-K aluminosilicate activity diagrams, calculated in GWB for the experimental conditions (150°C/75 bar), are presented in Figures 5a-c. In all diagrams, the fluid compositions lie within the stability fields of the end-member zeolite phases clinoptil-K, clinoptil-Ca, and mordenite-Na. Despite this, no evident zeolite phases were identified in the SEM observations. It is likely that the precipitation of amorphous silica was kinetically favoured over zeolite phases in both experiments. Their precipitation may also have been limited by the low temperature (150°C).

Figure 4a-c: Mineral saturations for the two experiments as calculated in GWB. Mineral saturations are shown for (a) amorphous silica, (b) calcite, and (c) anhydrite.

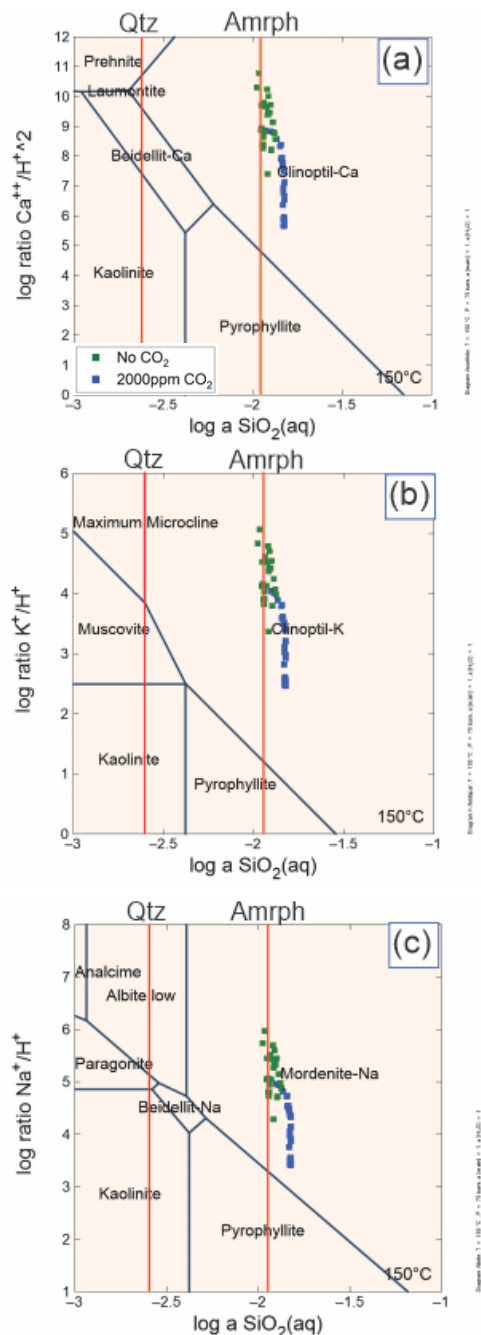
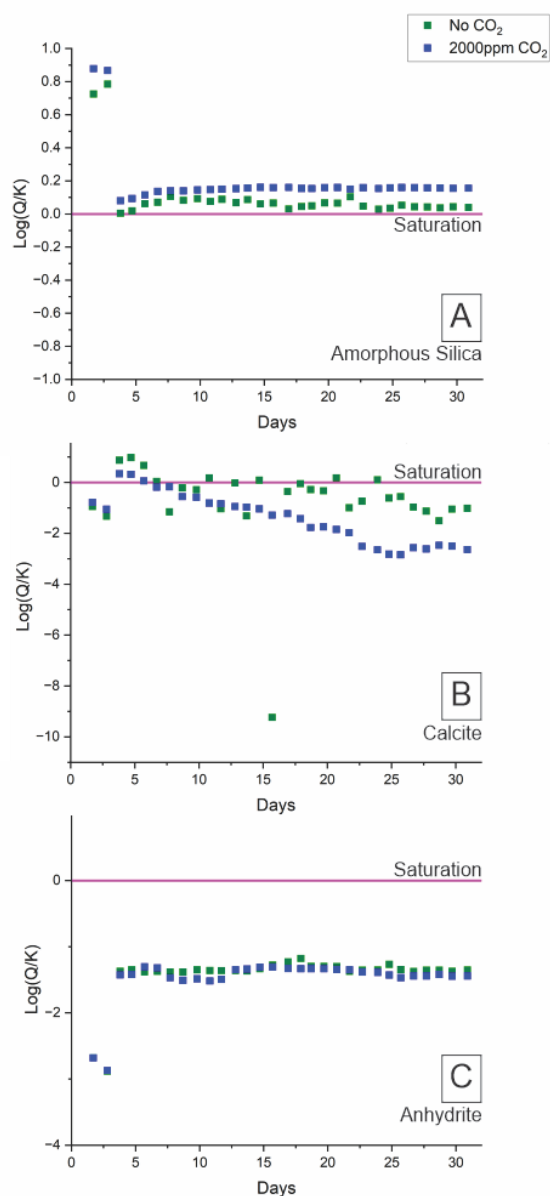


Figure 5a-c: Ca-Na-K aluminosilicate mineral activity-activity diagrams at 150°C and 75 Bars. Green points represent the experiment without CO₂ and blue points represent the experiment with 2000 ppm CO₂. These diagrams are produced using GWB. The red vertical lines show amorphous silica and quartz saturations at 150°C

5. CONCLUSION

We present the results of two experimental reinjection simulations conducted in high-PT flow-through reactors under geochemical conditions. These experiments investigated the effects of adding CO₂ to reinjection fluid, with a focus on silica scaling.

The first experiment aimed to observe the interaction between a typical acid-dosed reinjection brine and andesite with 1.5 wt.% calcite. This experiment revealed carbonate dissolution and reactions with minerals in the andesite, leading to increased pH and significant silica scaling. This was evident from both the SiO₂ concentrations in the effluent and SEM-EDS observations.

In the second experiment, 2000 ppm of CO₂ was added to the fluid under similar conditions (i.e., andesite with 1.5 wt.% calcite). This experiment demonstrated the capacity of CO₂ to buffer pH and inhibit silica scaling. SiO₂ loss in the effluent was minimal towards the end of the experiment, and SEM-EDS analysis showed little to no evidence of scaling.

Our results suggest that co-injection of CO₂ in geothermal power plants could be beneficial in reducing plant emissions and mitigating scaling within the reservoir in high salinity island-arc geothermal brines.

REFERENCES

- Bethke, C.M. (2022). *Geochemical and biogeochemical reaction modeling*. Cambridge University Press.
- Bethke, C.M., Farrell, B., Yeakel, S. (2018). *The Geochemist's workbench, version 12.0: GWB essentials guide*. Aqueous Solutions, LLC, Champaign, Illinois, US.
- Bethke, C.M., Farrell, B., Sharifironizoni, M. (2020). *GWB Reactive Transport Modeling Guide*.
- Bethke, C., Farrell, B., Sharifi, M. (2024). *The Geochemist's Workbench: Essentials Guide (Vol. 17)*. Aqueous Solutions, LLC.
- Defant, M. J., Maury, R., Joron, J., Feigenson, M. D., Leterrier, J., Bellón, H., Jacques, D., Richard, M. (1990). The geochemistry and tectonic setting of the northern section of the Luzon arc (The Philippines and Taiwan). *Tectonophysics*, 183(1-4), 187–205.
- Fan, K., Nam, S. (2018). Accelerating Geothermal Development in Indonesia: A Case Study in the Underutilization of Geothermal. *Consilience: The Journal of Sustainable Development* 19, 103-129.
- Fridriksson, T., Mateos, A., Audinet, P., Orucu, Y., (2016). Greenhouse gases from geothermal power production.
- Kaieda, H., Ueda A., Kubota K., Wakahama H., Mito S., Sugiyama K., Ozawa A., Kuroda Y., Sato H., Yajima T.: Field experiments for studying on CO₂ sequestration in solid minerals at the Ogachi HDR geothermal site, Japan. *Proc. 34th workshop on geothermal reservoir engineering*, Stanford University. (2009).
- Kaya, E., Zarrouk, S.J., (2017). Reinjection of greenhouse gases into geothermal reservoirs. *International Journal of Greenhouse Gas Control* 67, 111-129.
- Luo, W., Kottsova, A., Vardon, P. J., Dieudonné, A. C., Brehme, M. (2023). Mechanisms causing injectivity decline and enhancement in geothermal projects. *Renewable and Sustainable Energy Reviews*, 185.
- Montague, T., Stephenson, C., McLean, K., Brooks, A., Brotheridge, J., Pezaro, B., Allen, M., White, B., Zarrouk, S.J.: 2022 Annual Aotearoa New Zealand Geothermal Review Proc. 45th New Zealand Geothermal Workshop, Auckland, New Zealand. (2023).
- Mountain, B. W., Rendel, P., Sajkowski, L. (2022). CO₂ as an effective silica scaling inhibitor during reinjection of acid-dosed geothermal brines: An experimental study. *Goldschmidt 2022 Abstracts*.
- Nasridding, M., Ahamid, I., Daud, Y., Surachman, A., Sugiyono, A., Aditya, H. B., Mahlia T. M. I. (2016). Potential of geothermal energy for electricity generation in Indonesia: A review. *Renewable and Sustainable Energy Reviews* 53, 733-740.
- Passarella, M. (2021). *Basalt - fluid interactions at subcritical and supercritical conditions: An experimental study*. [Doctoral thesis, Victoria University of Wellington]. Open Access Te Herenga Waka-Victoria University of Wellington.
- Passarella, M., Mountain, B. W., Zarrouk, S. J., Burnell, J.: Experimental simulation of re-injection of non-condensable gases into geothermal reservoirs: greywacke-fluid interaction. *Proc. 37th New Zealand Geothermal Workshop*, Taupo, New Zealand. (2015).
- Purnomo, B. J., Pichler, T. (2014). Geothermal systems on the island of Java, Indonesia. *Journal of Volcanology and Geothermal Research* 285, 47–59.
- Rosenburg, M.D.: The Waitoa andesite (Kiwitahi Volcanic Group): a rediscovered volcano in the Hauraki Rift. Poster for the Geoscience New Zealand annual conference, Auckland. (2010).
- Sajkowski, L., Kamiya, A., Mountain, B.W. 2022. An experimental study on the potential of Rhenium and Indium as geothermal tracers. Lower Hutt (NZ): GNS Science. 33 p. (GNS Science report; 2022/23). doi: 10.21420/HNET-JY77
- Stimac, J. A., Nordquist, G., Suminar, A., Sirad-Azwar, L. (2008). An overview of the Awibengkok geothermal system, Indonesia. *Geothermics*, 37(3), 300–331.
- Sussman, D., Javellana, S. P., Benavidez, P. J. (1993). Geothermal energy development in the Philippines: An overview. *Geothermics*, 22(5–6), 353–367.